Journal of Luminescence 217 (2020) 116777

Contents lists available at ScienceDirect

Journal of Luminescence

journal homepage: http://www.elsevier.com/locate/jlumin

Largely enhanced elastico-mechanoluminescence of CaZnOS: Mn^{2+} by co-doping with Nd^{3+} ions

Min Su [a,b], Penghui Li [a,b], Shenghui Zheng [a,b], Xiaodan Wang [a,b], Junpeng Shi [a], Xia Sun [a], Hongwu Zhang [a,*]

[a] Key Lab of Urban Pollutant Conversion, Institute of Urban Environment, Chinese Academy of Sciences, Xiamen, 361021, China
[b] University of Chinese Academy of Sciences, No. 19A Yuquan Road, Beijing, 100049, China

ARTICLE INFO

Keywords:
Elastic-mechanoluminescence
Piezoelectric
Semiconducting
Sensor
Trap

ABSTRACT

In this paper, a large enhancement of red elastico-mechanoluminescence (EML) intensity has been observed in piezoelectric semiconducting CaZnOS: Mn^{2+} phosphors via the co-doping of Nd^{3+} ions. The optimal EML intensity of CaZnOS: 1%Mn^{2+}, 1.2%Nd^{3+} was about ten times than that of CaZnOS: 1%Mn^{2+}. In addition, the relationship between the EML intensity and the applied load was almost linear and the phosphor exhibited recoverable performance under ultraviolet (UV) (254 nm) excitation, which is a potential candidate for pressure sensing sensor applications. The thermoluminescence (TL) results indicated the co-doping of Nd^{3+} ions not only increased the concentration of traps but also introduced two new types traps. Further investigations revealed that the shallow trap contributed the most to the long afterglow and two deep traps were mainly responsible for the EML performance. Based on the piezoelectricity-induced detrapping model, all the results suggested the enhanced EML intensity of CaZnOS: Mn^{2+} can attribute to the increased trap quantity and regulated trap concentration generated by the co-doping of Nd^{3+} ions.

1. Introduction

Mechanoluminescence (ML) is a unique phenomenon in which various mechanical stimuli acting on solids are converted into light emission [1,2]. Although nearly 50% of inorganic salts and organic molecular solids exhibit ML during the fracture process, these materials play a limited role in practical applications due to the destructive nature of the process [3,4]. In the late 1990s, particularly the discovery of ZnS: Mn^{2+} (yellow) [5] and $SrAl_2O_4$: Eu^{2+} (green) [6] phosphors ignited the research upsurge of non-destructive elastic deformation ML also known as the elastico-mechanoluminescence (EML) [7]. As a subcategory of ML, it's worth noting that EML has numerous advantages, such as recoverability, intense luminance, and a precise linear relationship between light intensity and pressure providing real-time detection signals of stress in a reliable way, which can prompt the EML phosphors to be widely used in stress sensing, damage detection, engineering structure and human health monitoring sensors [8–13].

In recent years, although many EML phosphors have been developed, only a few can provide a sufficiently strong EML for detecting stress, most of which are based on piezoelectric materials such as ZnS, CaZnOS, (Ba,Ca)TiO_3 [5,14–16]. According to the currently accepted theory, the pressure-induced piezoelectric field of them can help to release trapped carriers, thereby emitting intense EML light. The research on CaZnOS has been a hot spot since its first discovery in 2003 [17]. It's worth noting that rare earth ions and transition metal ions can effectively replace the cation positions of Ca^{2+} and Zn^{2+}, respectively [14], so there have been many reports that CaZnOS are doped with different activators, which can emit various colors EML light. For example, green light emission can be observed from CaZnOS: Er^{3+} [10]. Wang et al. reported that Sm^{3+}-activated CaZnOS can emit red light [18]. Li's group found that CaZnOS: Nd^{3+} can effectively convert mechanical stress into near-infrared light penetrating deep into biological tissues [19]. Significantly, CaZnOS has been specifically identified as an excellent host lattice for Mn^{2+} due to its chemical and thermal stability properties, and thus has attracted the greatest attention in recent years [8,20–24]. In particular, Zhang and his colleagues have reported that CaZnOS: Mn^{2+} can emit strong red light under a variety of mechanical stimuli (ultrasonic vibration, impact, friction and compression) and its EML intensity increases linearly with the applied compression load and has recoverability, indicating the practical prospect on stress sensors [8].

* Corresponding author.
E-mail address: hwzhang@iue.ac.cn (H. Zhang).

https://doi.org/10.1016/j.jlumin.2019.116777
Received 7 July 2019; Received in revised form 23 September 2019; Accepted 24 September 2019
Available online 24 September 2019

Furthermore, CaZnOS: Mn^{2+} is a piezoelectric semiconductor with unique coupling physics, which can meet the integration application of piezoelectric semiconductor devices in the future [18]. However, although CaZnOS: Mn^{2+} has shown good potential in sensor applications, its EML intensity still needs to be further enhanced in order to increase the EML sensor sensitivity.

From previous reports, an effective way to enhance EML is to introduce suitable selected rare earth ions into the host matrix, which can slightly alter the symmetry of the crystal by chemical substitution, inducing changes in the piezoelectric field or modify the traps to ultimately improve the EML [7,15,25,26]. Up to now, Nd^{3+} ion's role in improving the intensity of EML is limited and how it works has not yet been definitely elucidated, which hinders the development of EML materials to some extent. Therefore, we synthesized a series of CaZnOS: Mn^{2+} phosphors with different Nd^{3+} contents by high-temperature solid-state reaction and investigated their EML properties. The results have revealed that the EML intensities were significantly improved when Nd^{3+} ions were introduced into CaZnOS: Mn^{2+}, and the best was about ten times better. The mechanism was discussed by combining the properties of photoluminescence (PL), long afterglow, EML and thermoluminescence (TL).

2. Experiment section

2.1. Sample preparation

A series of $Ca_{1-x}Zn_{0.99}OS$: $0.01Mn^{2+}$, xNd^{3+} (x = 0, 0.2%, 0.4%, 0.8%, 1.2%, 1.4%; the following are denoted as CaZnOS: Mn^{2+}, xNd^{3+} for simplicity) were synthesized via the traditional high-temperature solid-state method. The starting materials $CaCO_3$ (A.R.), ZnS (99.99%, Aladdin), $MnCO_3$ (99.95%, Aladdin), Nd_2O_3 (99.99%, Aladdin) were weighed in stoichiometric quantities and subsequently mixed and ground thoroughly in an agate mortar with moderate amounts of ethanol for 15–20 min. Then, the powders were transferred into alumina crucibles and sintered under an argon atmosphere at 1100 °C for 3 h. After that, the obtained materials were naturally cooled down to room temperature and reground for further measurements.

2.2. Characterizations

The phase purity and structure of the samples were identified using X-ray diffraction (XRD) (X′ Pert Pro PANalytical, Netherlands) operating at 40 kV and 40 mA with Cu Kα radiation (λ = 1.5406 Å) and the data were collected over the 2θ range from 10° to 80°. The morphology and elemental mapping of the CaZnOS: Mn^{2+}, 1.2%Nd^{3+} were measured by scanning electron microscopy (SEM, S-4800, Hitachi, Japan). The photoluminescence excitation (PLE) and emission spectra were recorded by using a fluorescence spectrometer (F-4600, Hitachi, Japan). The persistent luminescence properties of samples were measured by an Edinburgh FLS920 instrument. The ML measurements were observed by a lab-made system. Compression was produced using a universal testing machine (AGS-X, Shimadzu Corp.) and the ML intensity was monitored by a photon-counting system consisting of a photomultiplier tube (55777, Oriel Instruments) and a photon counter (C9692, Hamamatsu). The ML spectra were recorded with a photon multi-channel analyzer system (QE Pro-ABS). For evaluating the EML properties, the powder was mixed with an optical epoxy resin under a mass ratio of 1:9 to form pellet, which was solidified into a composite disk having a diameter of 25 mm and a thickness of 15 mm. The ML intensities and spectra were extracted by using optical fiber to collect light from a fixed spot, which was 1 cm close to the position of the disk's contact point with the mechanical testing machine. The thermoluminescence (TL) was measured by combining a fluorescence spectrometer (FLS920, Edinburgh) with a laboratory-made temperature control device including a nitrogen bath cryostat (Optistat DN, Oxford Instruments) and a temperature controller (Intelligent temperature controller, Oxford Instruments). In the heating stage, the powders weighed for the same mass (20 mg) were heated from 273.5 K to 500 K at a heating rate of 10 K/min. Prior to the ML and TL tests, these samples were first exposed to ultraviolet (UV) lamp (254 nm, 6 W) for 3 min and then stopped for different decay times (3 min and 0.5 h). All measurements except TL were performed at room temperature.

3. Results and discussion

3.1. Phase and crystal structure of CaZnOS: Mn^{2+}, Nd^{3+}

Fig. 1(a) shows the XRD patterns of CaZnOS: Mn^{2+}, xNd^{3+} along with different Nd^{3+} contents. Compared with the standard ICSD card of CaZnOS (No: 245309), it can be observed that all the samples were pure CaZnOS phase combined and the dopants of Nd^{3+} did not change its structure. As the previous reports [15,17,27], the crystal structure of the CaZnOS is a noncentrosymmetric type structure which fits in the hexagonal system in the space group $P6_3mc$, presenting an excellent piezoelectricity. The typical structure of CaZnOS is shown in Fig. 1(b). It can be seen that each Zn atom is surrounded by three S atoms and one O atom to form a ZnS_3O tetrahedron and the tetrahedra are all aligned parallel, resulting in a polar structure. The coordination environment of Ca atoms is an octahedron composed of three S atoms and three Zn atoms. Considering the matching of coordination number (CN) and ionic radii (Å), the doped Mn^{2+} (CN4, 0.66 Å) ions and Nd^{3+} (CN6, 0.98 Å) ions are prone to replace the positions of Zn^{2+} (CN4, 0.60 Å) and Ca^{2+} (CN6, 1.00 Å), respectively [19,21]. Due to the difference between the size of ionic radii and the electronegativity, the replacement of Nd^{3+} for Ca^{2+} can not only create the $V_{Ca}^{''}$ but also can result in the lower symmetry of CaZnOS structure. As reported in previous lectures, the EML performances are closely related with the trap number and structure symmetry [7,15,25,26]. Thus, the co-doping of Nd^{3+} plays an important effect on the EML intensity of CaZnOS: Mn^{2+}.

The morphology and elemental mapping characterizations of the CaZnOS: Mn^{2+}, 1.2%Nd^{3+} are depicted in Fig. 2(a)–(h). As can be seen from Fig. 2(a) and (b), the sample consisted of small, roughened spherical grains with a size smaller than 10 μm, which closely clustered together. In addition, energy dispersive spectroscopy (EDS) elemental mapping images (Fig. 2 (c)–(h)) indicate that Ca, Zn, O, S, Mn and Nd atoms were evenly distributed throughout the selected portion, suggesting that the formation of CaZnOS: Mn^{2+}, Nd^{3+}.

3.2. The effect of co-doping Nd^{3+} on photoluminescence properties of CaZnOS: Mn^{2+}

Fig. 3 (a) demonstrates the PLE spectra of samples with different Nd^{3+} concentrations. The former excitation band centered at ~282 nm, which can be ascribed to the excitation band of the host lattice [21]. And other excitation peaks located approximately at 398 nm, 434 nm, 496 nm and 512 nm can be attributed to the electronic transitions of Mn^{2+} from ground-level $^6A_1(^6S)$ to the $^4T_2(^4D)$, [$^4A_1(^4G)$, $^4E(^4G)$], $^4T_2(^4G)$ and $^4T_1(^4G)$, respectively. Obviously, the intensity of the host lattice excitation band is much stronger than the latter, indicating that the energy was transferred effectively from the host lattice to Mn^{2+}. And this resulted in the typical emission of Mn^{2+} [20,21]. The emission spectra of the samples showed a broad orange-red emission band. The stronger peak located at ~605 nm can be ascribed to $^4T_1(^4G)$-$^6A_1(^6S)$ transition of Mn^{2+}. And there was a weak emission band located at ~530 nm, which is properly attributed to the defect centers formed by Mn^{2+} doping (Fig. 3 (b)) [21]. It should be noted that Nd^{3+} co-doping did not alter the shapes of excitation and emission spectra. However, with the increase of the doping amount, the intensities of PLE and PL weaken gradually, which indicated that the defects created by Nd^{3+} co-doping can be regarded as the traps centers to capture the excited carriers and thus inhibit the PL intensity.

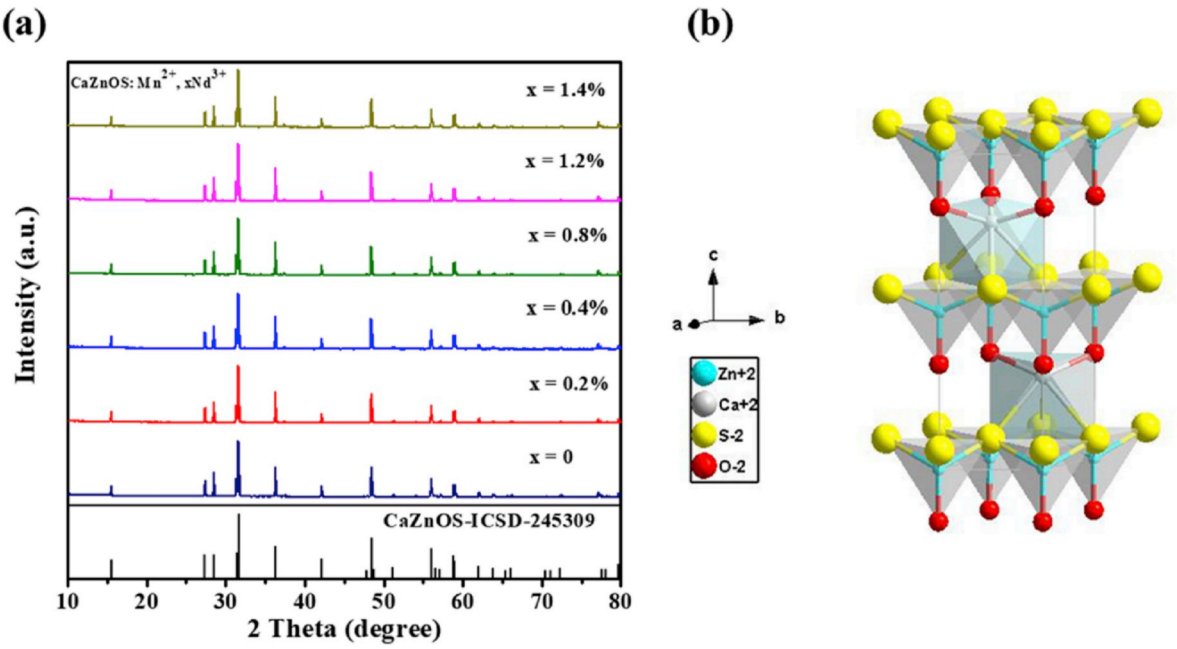

Fig. 1. (a) XRD patterns of the CaZnOS: Mn^{2+}, xNd^{3+} (x = 0, 0.2%, 0.4%, 0.8%, 1.2%, 1.4%) samples; (b) Schematic presentation of crystal structure of CaZnOS.

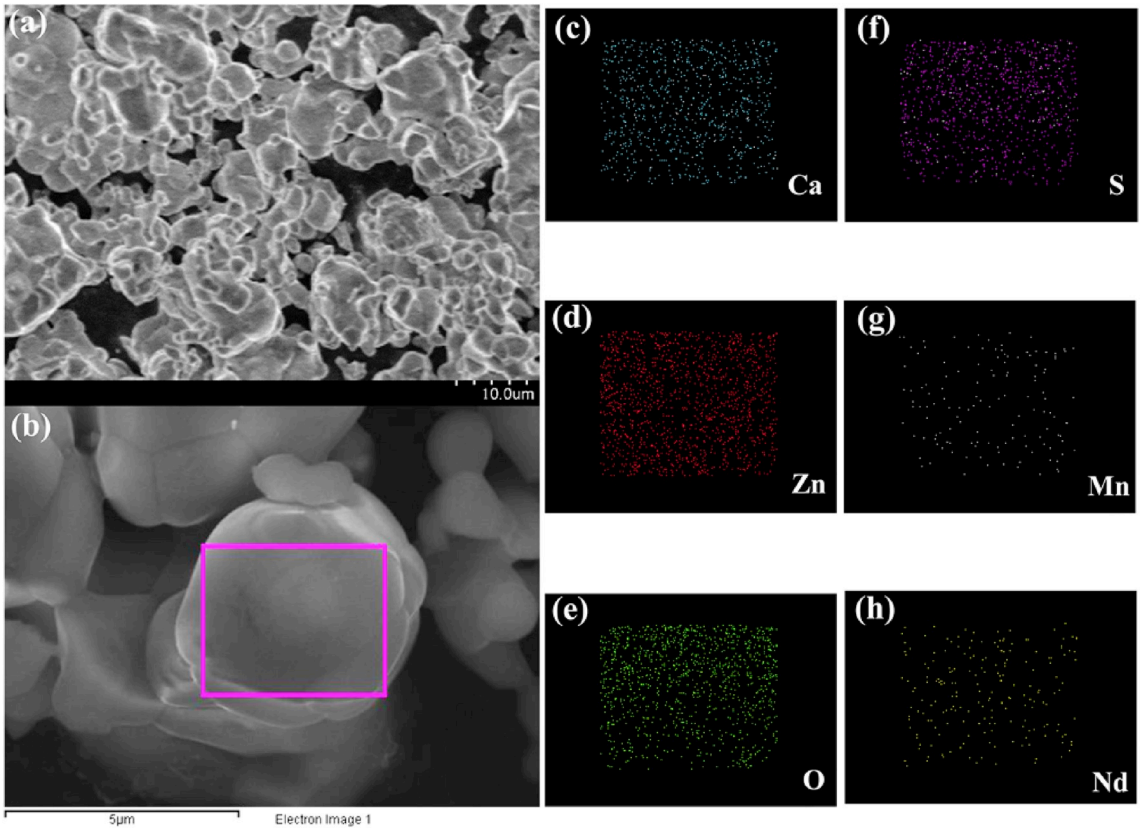

Fig. 2. SEM images of the CaZnOS: Mn^{2+}, 1.2%Nd^{3+} (a), (b) and related EDS elemental mapping images of Ca (c), Zn (d), O (e), S (f), Mn (g) and Nd (h).

The previous lectures have confirmed that the afterglow properties of the phosphors have certain correlation with their EML intensities [26,28,29]. Therefore, the effect of Nd^{3+} content on the afterglow properties of CaZnOS: Mn^{2+} has been investigated, as shown in Fig. 4. All the afterglow emission peaks were similar, which were mainly located at 625 nm. Compared with the emission spectra, the peak located at 530 nm was very weak in the afterglow emission. The above results indicated that the afterglow emission mainly comes from the $^4T_1(^4G)$ to $^6A_1(^6S)$ transition of Mn^{2+} that peaked at approximately 625 nm. At the same time, the co-doping of Nd^{3+} markedly increased the afterglow intensity of CaZnOS: Mn^{2+} by about one order of magnitude and the sample with 1.2% Nd^{3+} concentration showed the best persistent

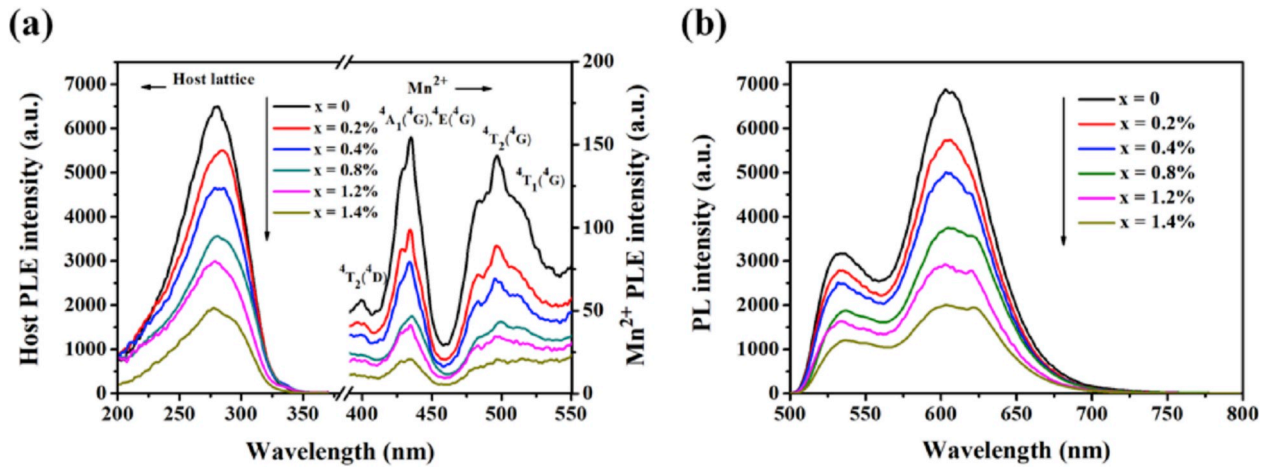

Fig. 3. (a) PLE ($\lambda_{em} = 605$ nm) and (b) PL ($\lambda_{ex} = 282$ nm) spectra of the CaZnOS: Mn^{2+}, xNd^{3+} (x = 0, 0.2%, 0.4%, 0.8%, 1.2%, 1.4%).

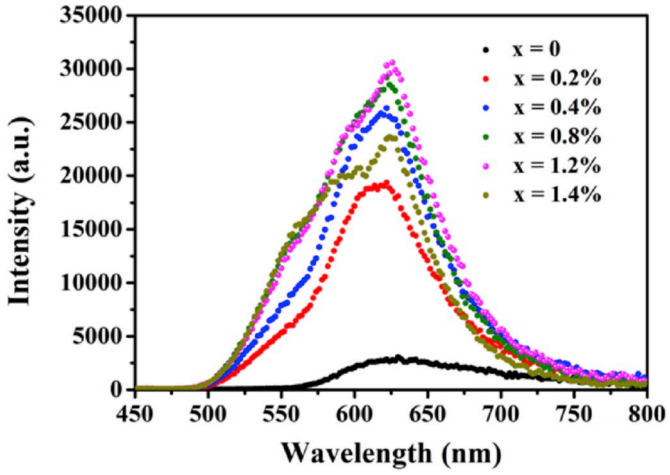

Fig. 4. Afterglow spectra of the CaZnOS: Mn^{2+}, xNd^{3+} (x = 0, 0.2%, 0.4%, 0.8%, 1.2%, 1.4%) after UV (254 nm) irradiation for 3 min and then a delay of 10 s.

performance, suggesting the Nd^{3+} ions into the host lattice produce more traps centers.

3.3. The effect of co-doping Nd^{3+} on EML properties of CaZnOS: Mn^{2+}

In order to investigate the effects of Nd^{3+} co-doping on EML performance, a compressive load up to 1000 N was imposed on all samples at a constant rate of 10 mm/min. The EML measurements were conducted following a previously described method [30,31]. The EML properties of the samples doped with Nd^{3+} at different concentrations are shown in Fig. 5 (a). Firstly, there was almost a linear relationship between the EML intensities of all the samples and the applied compressive loads, indicating that the as-prepared samples can be used to detect the stress. Furthermore, the EML intensity of CaZnOS: Mn^{2+} enhanced with the increase of Nd^{3+} content and the largest EML intensity was obtained in the sample with x = 1.2%, about 10 times than that of CaZnOS: Mn^{2+} in compression load of 1000 N, which was consistent with the improvement of afterglow intensity ((Fig. 5 (b)). Fig. 5 (c) shows the EML response of CaZnOS: Mn^{2+}, 1.2%Nd^{3+} under five repetitive load circles. For each cycle, the EML intensity increased linearly with the applied load, and the highest EML intensity corresponded to the peak of the applied force. However, the EML intensity decreased quickly following the increase of circle, which can be attributed to the de-trapping process of trapped carriers [26]. More importantly, the EML intensity recovered again when the sample was re-excited by the UV lamp (254 nm). The recovery remained stable even repeated for 5 times (Fig. 5 (d)). It is concluded that the performance of EML is not damaged by repeated compression and further confirmed the traps play an important effect on EML intensity of the CaZnOS: Mn^{2+}. The good linear correlation and recoverable properties suggested that CaZnOS: Mn^{2+}, Nd^{3+} is a potential sensor material for detecting stress and damage. From Fig. 5(e), it can be observed that the EML spectrum was almost identical to the afterglow spectrum and there was merely one peak at 625 nm from the $^4T_1(^4G)$ to $^6A_1(^6S)$ transition of Mn^{2+} (Fig. 5 (e)). Therefore, the EML of CaZnOS: Mn^{2+}, Nd^{3+} is also originated from the Mn^{2+} center.

Obviously, the peak intensity of PL spectrum was different from that of afterglow spectrum and EML spectrum at ~530 nm. The similar situations have been found in some EML materials, such as $SrAl_2O_4$: Ce^{3+}, Ho^{3+} [32], (Sr, Ca, Ba)$_2$ SnO_4: Sm^{3+}, La^{3+} [33]. It may be related to electrons transfer and the way energy is transmitted to the emission center Mn^{2+}. The precise reason needs to be further investigated.

3.4. The possible effect mechanism of Nd^{3+} co-dopant on the EML of CaZnOS: Mn^{2+}

The previous reports have proved that the traps existing in the phosphors play a dominant role on their EML intensities [7,34,35]. The thermoluminescence (TL) curves of all examples monitored at 625 nm were utilized to evaluate their trap properties, as shown in Fig. 6. For CaZnOS: Mn^{2+} sample, there was only a weak peak temperature at around 309 K. By analyzing and combining the results of previous studies [15,36,37], it indicated that the existence of solely one TL peak is mainly created by the native point defect in CaZnOS. With the increase of Nd^{3+} content, the TL peaks located at higher temperatures appeared, which indicated that the traps with deeper trap depth have been created. Many researches have confirmed that replacing the low-valent metal ions with the high-valent metal ions would produce some defects acting as traps [31,38], so probably because the charge compensation between the Nd^{3+} and Ca^{2+} ions occurs:

$$2Nd^{3+} + 3Ca2 + \rightarrow 2Nd^{\cdot}_{Ca} + V^{''}_{Ca} \quad (1)$$

The $Nd^{\cdot}_{Ca}$ carries positive charge as electron traps and a simultaneous creation of negative defect $V^{''}_{Ca}$, which acts as hole traps, resulting in the TL curves have two more peaks compared to the one without Nd^{3+} ions. In addition, the TL intensity was dramatically increased with the increase of Nd^{3+} content, reaching the maximum value for 1.2% of Nd^{3+}, afterward, which suggested that higher concentration of traps have been created via the co-doping of Nd^{3+}. This TL results were consistent with the afterglow and EML results, further indicating that the trap type and

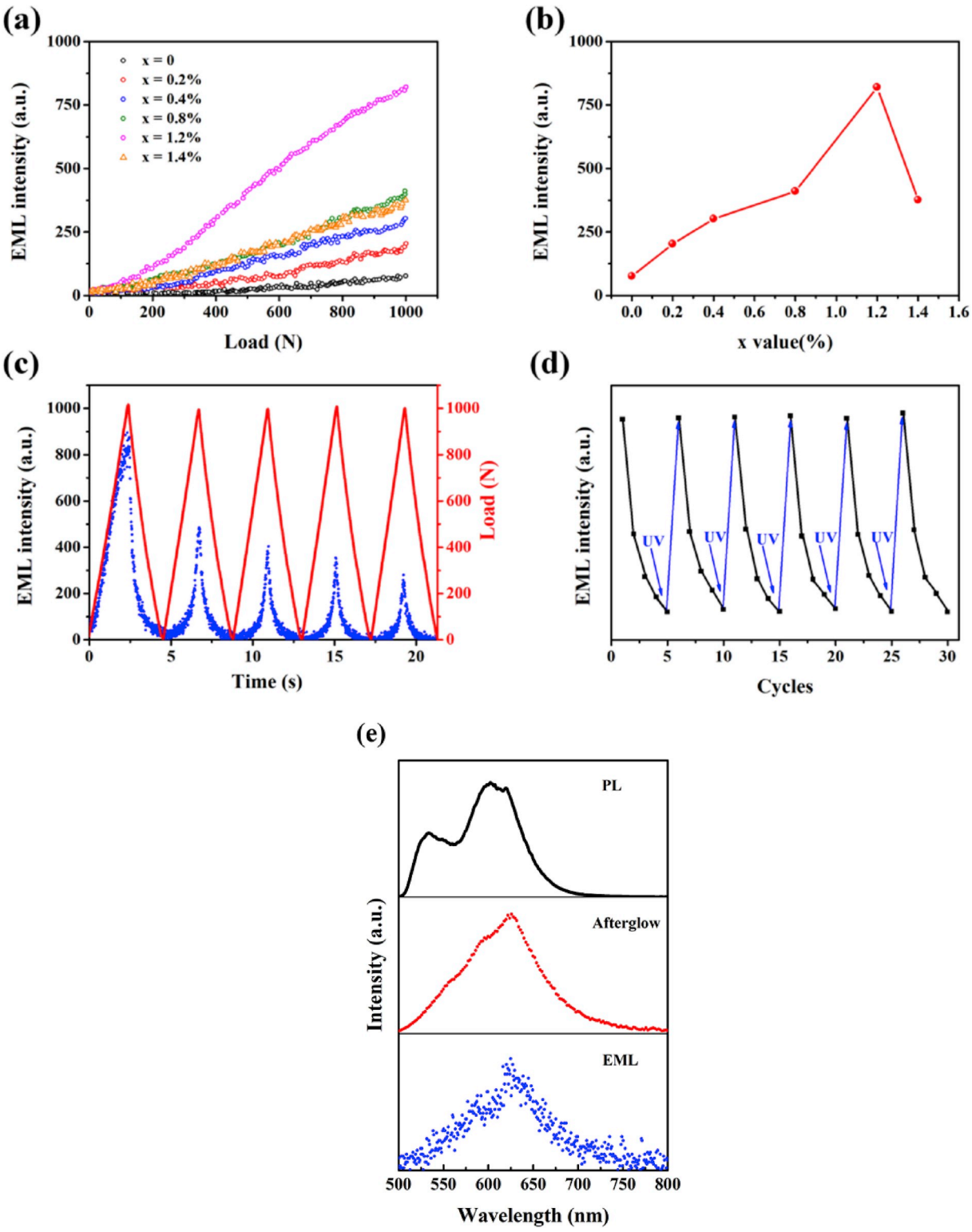

Fig. 5. (a) Comparison of EML intensities for the CaZnOS: Mn^{2+}, Nd^{3+} with different Nd^{3+} doping contents; (b) EML intensity dependence on x value, in compression load of 1000 N; (c) EML response of the CaZnOS: Mn^{2+}, 1.2%Nd^{3+} under five repeated pressure; (d) EML recovery behavior after UV irradiation; (e) PL, afterglow and EML spectra of the CaZnOS: Mn^{2+}, 1.2%Nd^{3+}.

concentration have important effects on EML.

In order to investigate the effect of different traps on EML properties of CaZnOS: Mn^{2+}, Nd^{3+}, the TL curve of CaZnOS: Mn^{2+}, 1.2%Nd^{3+} was decomposed into three peaks located at 297, 328 and 375 K, respectively, according to the Gaussian function shown in Fig. 7 (a). The depths of different traps can be estimated by the following equations [39,40]:

$$E = T_m/500 \quad (2)$$

where E is the trap depth and T_m is the maximum peak temperature of the TL curve. The traps depths corresponding to peak 1, peak 2 and peak 3 were 0.594 eV, 0.656 eV and 0.75 eV, respectively. To further

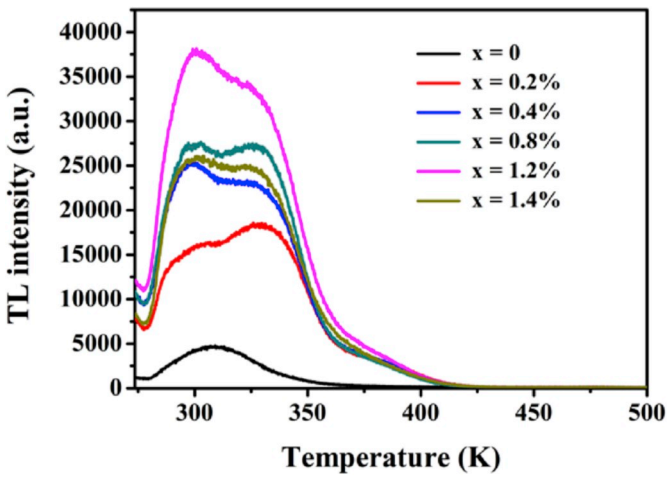

Fig. 6. Comparatively TL glow curves of CaZnOS: Mn^{2+}, xNd^{3+} monitored at 625 nm with a heating rate of 10 K/min.

understand the deep trap, the TL curve of the same sample was measured at a delay time of 30 min, as shown in Fig. 7 (b). It should be noted that the shallow trap with 0.594 eV trap depth decreased greatly while two deep traps only lowered a little. Furthermore, we also measured the EML intensity after different delay time (Fig. 7 (c)). It can be noted that the EML intensities of the sample after 3 min and 30 min were nearly identical. Combination of the afterglow, TL and EML results, it can be found that the shallow trap was mainly responsible for the long afterglow emission and the deep traps induced the strong EML intensity. In conclusion, the co-doping Nd^{3+} created a large number of deep traps, which answered for the obvious increase of EML intensity for CaZnOS: Mn^{2+}.

It was known from previous reports [15,41] that CaZnOS is a piezoelectric semiconductor, suggesting that CaZnOS can produce strong piezoelectric field when a load is applied on it. In this way, the trapped electrons would be excited from the traps and produce EML. Thus, the piezoelectricity-induced detrapping model was utilized to explore the possible effect mechanism of Nd^{3+} co-doping on the EML of CaZnOS: Mn^{2+}, as shown in Fig. 8. According to previous study [42], the electronic energy level structure of Mn^{2+} ion is deep under the valence band, so we put them beside the band diagram. Under UV irradiation, electrons are excited to the conduction band (CB) and spontaneously holes are generated (progress ①). The absorbed energy is transmitted to Mn^{2+} ions via the host lattice, resulting in the $^4T_1(^4G)$ to $^6A_1(^6S)$ transition of Mn^{2+} (progress ②) [21]. In addition, a large number of electrons are captured by different traps in the lattice defects (progress ③),

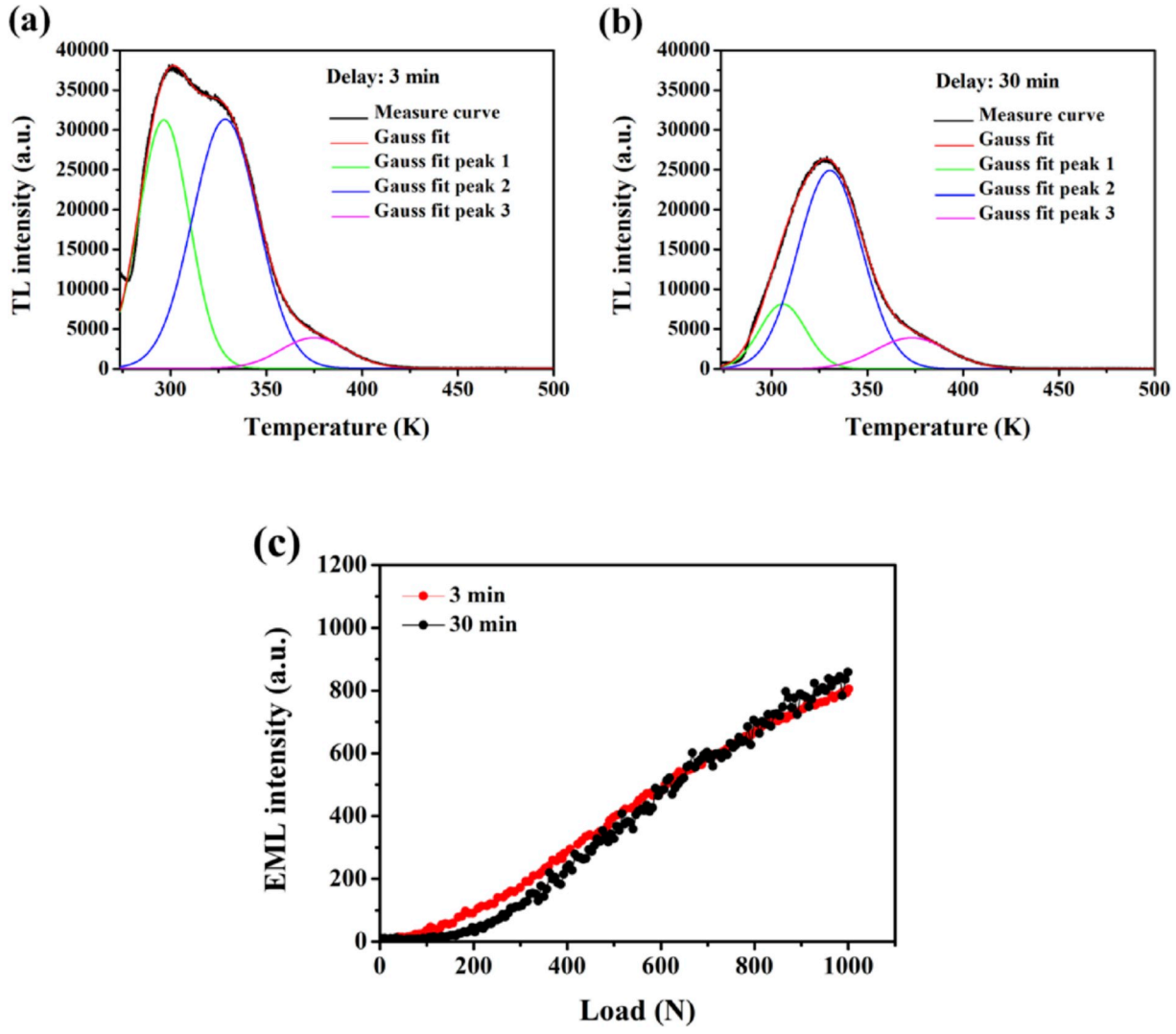

Fig. 7. TL glow curves and Gaussian fits of CaZnOS: Mn^{2+}, 1.2%Nd^{3+} at (a) 3 min and (b) 30 min after UV irradiation for 3 min; (c) EML response of the CaZnOS: Mn^{2+}, 1.2%Nd^{3+} after different delay time.

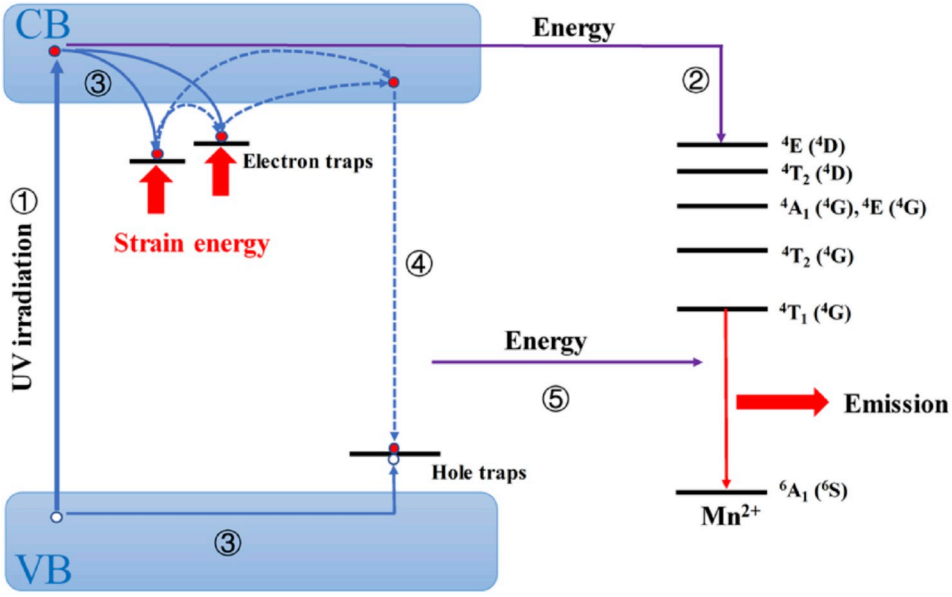

Fig. 8. The schematic diagram of elastico-mechanoluminescence (EML) mechanism in CaZnOS: Mn^{2+}, Nd^{3+}. CB: conduction band, VB: valence band.

once a stress is utilized, the host lattice is deformed, and a local electric field is generated in the piezoelectric region. The trapped carriers are released to the CB under the action of the piezoelectric field, and then non-radiative recombination with the holes is generated (progress ④), followed by the energy is transferred to the luminescence center Mn^{2+} ions [8], which is excited to emit red light at a wavelength of 625 nm (progress ⑤). The introduced Nd^{3+} ions generate a large number of deep traps, which can effectively capture the electrons and result in stronger EML emission.

4. Conclusions

In summary, we synthesized a series of CaZnOS: Mn^{2+}, xNd^{3+} ($x = 0$, 0.2%, 0.4%, 0.8%, 1.2%, 1.4%) phosphors via high-temperature solid-state reaction. The EML intensity of CaZnOS: Mn^{2+} was greatly increased by one order of magnitude with the content of Nd^{3+} ions were 1.2%. Furthermore, the EML intensity increased linearly with the applied load, suggesting that CaZnOS: Mn^{2+}, Nd^{3+} has good potential as a detecting pressure and damage sensor. The long afterglow and TL have confirmed that co-doping of Nd^{3+} not only produced two deep traps but also enhanced the concentration of traps obviously. The three traps depths of CaZnOS: Mn^{2+}, 1.2%Nd^{3+} were estimated to be 0.594, 0.656 and 0.75 eV, respectively. And the obtained results revealed that trap 1 contributed the most to long afterglow while trap 2 and 3 was mainly responsible for the performance of EML. Based on the piezoelectricity-induced detrapping model, the increased trap concentration induced by the co-doping Nd^{3+} ions should be answered for the enhancement of its EML intensity.

Acknowledgements

This work was supported by sensitivity the Key Program of International Cooperation of Fujian Province (2019I0032).

References

[1] B.P. Chandra, Mechanoluminescence (1998) 361.
[2] B.P. Chandra, A.S. Rathore, Classification of mechanoluminescence, Cryst. Res. Technol. 30 (1995) 885–896.
[3] B.P. Chandra, V.K. Chandra, P. Jha, Microscopic theory of elastico-mechanoluminescent smart materials, Appl. Phys. Lett. 104 (2014), 031102.
[4] S.W. Shin, J.P. Oh, C.W. Hong, E.M. Kim, J.J. Woo, G.-S. Heo, J.H. Kim, Origin of mechanoluminescence from Cu-doped ZnS particles embedded in an elastomer film and its application in flexible electro-mechanoluminescent lighting devices, ACS Appl. Mater. Interfaces 8 (2016) 1098–1103.
[5] C.N. Xu, T. Watanabe, M. Akiyama, X.G. Zheng, Artificial skin to sense mechanical stress by visible light emission, Appl. Phys. Lett. 74 (1999) 1236–1238.
[6] C.N. Xu, T. Watanabe, M. Akiyama, X.G. Zheng, Direct view of stress distribution in solid by mechanoluminescence, Appl. Phys. Lett. 74 (1999) 2414–2416.
[7] J.C. Zhang, X.S. Wang, G. Marriott, C.N. Xu, Trap-controlled mechanoluminescent materials, Prog. Mater. Sci. 103 (2019) 678–742.
[8] J.C. Zhang, C.N. Xu, S. Kamimura, Y. Terasawa, H. Yamada, X.S. Wang, An intense elastico-mechanoluminescence material CaZnOS: Mn^{2+} for sensing and imaging multiple mechanical stresses, Opt. Express 21 (2013) 12976–12986.
[9] J.C. Zhang, Y.Z. Long, X. Yan, X.S. Wang, F. Wang, Creating recoverable mechanoluminescence in piezoelectric calcium niobates through Pr^{3+} doping, Chem. Mater. 28 (2016) 4052–4057.
[10] H.L. Zhang, D.F. Peng, W. Wang, L. Dong, C.F. Pan, Mechanically induced light emission and infrared-laser-induced upconversion in the Er-doped CaZnOS multifunctional piezoelectric semiconductor for optical pressure and temperature sensing, J. Phys. Chem. C 119 (2015) 28136–28142.
[11] Y. Fujio, C.N. Xu, Y. Terasawa, Y. Sakata, J. Yamabe, N. Ueno, N. Terasaki, A. Yoshida, S. Watanabe, Y. Murakami, Sheet sensor using $SrAl_2O_4$: Eu mechanoluminescent material for visualizing inner crack of high-pressure hydrogen vessel, Int. J. Hydrogen Energy 41 (2016) 1333–1340.
[12] S. Timilsina, K.H. Lee, Y.N. Kwon, J.S. Kim, Optical evaluation of in situ crack propagation by using mechanoluminescence of $SrAl_2O_4$: Eu^{2+}, Dy^{3+}, J. Am. Ceram. Soc. 98 (2015) 2197–2204.
[13] W.Z. Wu, X.N. Wen, Z.L. Wang, Taxel-addressable matrix of vertical-nanowire piezotronic transistors for active and adaptive tactile imaging, Science 340 (2013) 952–957.
[14] Y.Y. Du, Y. Jiang, T.Y. Sun, J.X. Zhao, B.L. Huang, D.F. Peng, F. Wang, Mechanically excited multicolor luminescence in lanthanide ions, Adv. Mater. 31 (2019) 1807062.
[15] C. Pan, J.C. Zhang, M. Zhang, X. Yan, Y.Z. Long, X.S. Wang, Intrinsic oxygen vacancies mediated multi-mechano-responsive piezoluminescence in undoped zinc calcium oxysulfide, Appl. Phys. Lett. 110 (2017) 233904.
[16] X.S. Wang, C.N. Xu, H. Yamada, K. Nishikubo, X.G. Zheng, Electro-mechano-optical conversions in Pr^{3+}-doped $BaTiO_3$-$CaTiO_3$ ceramics, Adv. Mater. 17 (2005) 1254–1258.
[17] S.A. Petrova, V.P. Mar'evich, R.G. Zakharov, E.N. Selivanov, V.M. Chumarev, L. Y. Udoeva, Crystal structure of zinc calcium oxysulfide, Dokl. Chem. 393 (2003) 255–258.
[18] W. Wang, D.F. Peng, H.L. Zhang, X.H. Yang, C.F. Pan, Mechanically induced strong red emission in samarium ions doped piezoelectric semiconductor CaZnOS for dynamic pressure sensing and imaging, Opt. Commun. 395 (2017) 24–28.
[19] L.J. Li, L. Wondraczek, L.H. Li, Y. Zhang, Y. Zhu, M.Y. Peng, C.B. Mao, CaZnOS, Nd^{3+} emits tissue-penetrating near-infrared light upon force loading, ACS Appl. Mater. Interfaces 10 (2018) 14509–14516.
[20] C.J. Duan, A.C.A. Delsing, H.T. Hintzen, Photoluminescence properties of novel red-emitting Mn^{2+}-activated MZnOS (M = Ca, Ba) Phosphors, Chem. Mater. 21 (2009) 1010–1016.
[21] J.C. Zhang, L.Z. Zhao, Y.Z. Long, H.D. Zhang, B. Sun, W.P. Han, X. Yan, X.S. Wang, Color manipulation of intense multiluminescence from CaZnOS: Mn^{2+} by Mn^{2+} concentration effect, Chem. Mater. 27 (2015) 7481–7489.

[22] Z.H. Xu, Z.G. Xia, B.F. Lei, Q.L. Liu, Full color control and white emission from CaZnOS: Ce^{3+}, Na^{+}, Mn^{2+} phosphors via energy transfer, J. Mater. Chem. C 4 (2016) 9711–9716.
[23] J.J. Joos, K. Lejaeghere, K. Korthout, A. Feng, D. Poelman, P.F. Smet, Charge transfer induced energy storage in CaZnOS: Mn-insight from experimental and computational spectroscopy, Phys. Chem. Chem. Phys. 19 (2017) 9075–9085.
[24] B.L. Huang, D.F. Peng, C.F. Pan, Energy Relay Center" for doped mechanoluminescence materials: a case study on Cu-doped and Mn-doped CaZnOS, Phys. Chem. Chem. Phys. 19 (2017) 1190–1208.
[25] L. Zhang, C.N. Xu, H. Yamada, N. Bu, Enhancement of mechanoluminescence in $CaAl_2Si_2O_8$: Eu^{2+} by partial Sr^{2+} substitution for Ca^{2+}, J. Electrochem. Soc. 157 (2010) J50–J53.
[26] J.C. Zhang, Y.Z. Long, X.S. Wang, C.N. Xu, Controlling elastico-mechanoluminescence in diphase (Ba,Ca)TiO_3: Pr^{3+} by co-doping different rare earth ions, RSC Adv. 4 (2014) 40665–40675.
[27] T. Sambrook, C.F. Smura, S.J. Clarke, K.M. Ok, P.S. Halasyamani, Structure and physical properties of the polar oxysulfide CaZnOS, Inorg. Chem. 46 (2007) 2571–2574.
[28] H. Fang, G.J. Qiu, J. Li, X.S. Wang, Sr^{2+} substitution for Ca^{2+} and Eu^{2+}, Dy^{3+} co-doping enhance mechanoluminescence of $CaAl_2Si_2O_8$ phosphors, J. Alloy. Comp. 763 (2018) 267–272.
[29] G.J. Qiu, H. Fang, X.S. Wang, Y.X. Li, Largely enhanced mechanoluminescence properties in Pr^{3+}/Gd^{3+} co-doped $LiNbO_3$ phosphors, Ceram. Int. 44 (2018) 15411–15417.
[30] X.Y. Fu, S.H. Zheng, J.P. Shi, H.W. Zhang, Enhanced blue mechanoluminescence of $Sr_nMgSi_2O_{5+n}$: Eu alkali-earth silicate induced by defective phase, J. Lumin. 192 (2017) 117–122.
[31] X.Y. Fu, S.H. Zheng, J.P. Shi, Y.N. Liu, X.Y. Xu, H.W. Zhang, Investigation of the cyan phosphor $Ba_2Zr_2Si_3O_{12}$: Eu^{2+}, Dy^{3+}: mechanoluminescence properties and mechanism, J. Alloy. Comp. 766 (2018) 221–228.
[32] H.W. Zhang, H. Yamada, N. Terasaki, C.N. Xu, Ultraviolet mechanoluminescence from $SrAl_2O_4$: Ce and $SrAl_2O_4$: Ce, Ho, Appl. Phys. Lett. 91 (2007), 081905.
[33] H.F. Zhao, X. N Chai, X.S. Wang, Y.X. Li, X. Yao, Mechanoluminescence in (Sr,Ca,Ba)$_2SnO_4$: Sm^{3+}, La^{3+} ceramics, J. Alloy. Comp. 656 (2016) 94–97.
[34] P.X. Xiong, M.Y. Peng, Near infrared mechanoluminescence from the Nd^{3+} doped perovskite $LiNbO_3$: Nd^{3+} for stress sensors, J. Mater. Chem. C 7 (2019) 6301–6307.
[35] P.X. Xiong, M.Y. Peng, J.K. Cao, X.L. Li, Near infrared mechanoluminescence from $Sr_3Sn_2O_7$: Nd^{3+} for in situ biomechanical sensor and dynamic pressure mapping, J. Am. Ceram. Soc. 102 (2019) 5899–5909.
[36] B.L. Huang, Energy harvesting and conversion mechanisms for intrinsic upconverted mechano-persistent luminescence in CaZnOS, Phys. Chem. Chem. Phys. 18 (2016) 25946–25974.
[37] Y.J. Zheng, H.M. Zhang, H.R. Zhang, X.J. Zhang, Y.L. Liu, B.F. Lei, Enhanced persistent properties of Mn^{2+} activated CaZnOS, RSC Adv. 7 (2017) 38498–38505.
[38] H.D. Luo, A.J.J. Bos, P. Dorenbos, Controlled electron-hole trapping and detrapping Process in $GdAlO_3$ by valence band engineering, J. Phys. Chem. C 120 (2016) 5916–5925.
[39] J.T. Randall, M.H.F. Wilkins, Phosphorescence and electron traps-I. The study of trap distributions, Proc. R. Soc. Lond. 184 (1945) 366–389.
[40] D.D. Zhou, Z.Z. Wang, Z. Song, F.X. Wang, S.Y. Zhang, Q.L. Liu, Enhanced persistence properties through modifying the trap depth and density in $Y_3Al_2Ga_3O_{12}$: Ce^{3+}, Yb^{3+} Phosphor by Co-doping B^{3+}, Inorg. Chem. 58 (2019) 1684–1689.
[41] P.C. Ricci, J. Satta, D. Chiriu, R. Corpino, C.M. Carbonaro, M. Salis, C. Melis, P. S. Normile, J.A. De Toro, Optical and vibrational properties of CaZnOS: the role of intrinsic defects, J. Alloy. Comp. 777 (2019) 225–233.
[42] J. Planelles-Aragó, B. Julián-López, E. Cordoncillo, P. Escribano, F. Pellé, B. Viana, C. Sanchez, Lanthanide doped ZnS quantum dots dispersed in silica glasses: an easy one pot sol-gel synthesis for obtaining novel photonic materials, J. Mater. Chem. 18 (2008) 5193–5199.